PHILIPPINE ENGINEERING JOURNAL
PEJ 2025; Vol. 46, No. 1: 88-100

Received: 20 November 2024
Received in Revised Form: 4 February 2025
Accepted: 6 May 2025

Comparing Analytical and AI-based Image Analysis for Micron-sized Particle Detection and Measurement

Anton Justo P. Ventura[1]***, Tristan Ahmad A. Harun***[2]***, Carl James M. Kimayong***[3]***, Candy C. Mercado***[1*]
[1]*Department of Mining, Metallurgical, and Materials Engineering, College of Engineering, University of the Philippines Diliman, Quezon City, Philippines*
[2]*Philippines Science High School - Cordillera Administrative Region Campus, Philippines*
[3]*Philippine Science High School - Cagayan Valley Campus, Bayombong, Nueva Vizcaya, Philippines*
**Corresponding author: ccmercado1@up.edu.ph*

Abstract *– Microscopy is the study of analyzing cells and molecules at the microscopic level using tools such as light microscopes. Images from the microscope are imported into image analysis software to further evaluate the cell count and measurements of the cell. Artificial intelligence is being utilized in microscopy for faster analysis of cells, allowing researchers to train the software to recognize specific cells and molecules. Analytical and artificial image analysis programs, using FIJI/ImageJ and Polygon AI respectively, are compared by their ability to analyze chitosan and gold microparticles, as well as compare the speed and accuracy of the software's identification and modeling. Results show that the Polygon AI software fares better at cell detection where the pre-trained Somatic model fares over FIJI/ImageJ yielding up to 97% true positive count for chitosan and 90% true positive count for gold microparticles. FIJI/ImageJ fares better at reporting cell measurements, where the region of interest (ROI) borders fully encapsulate the cell compared to Polygon AI with diameter measurement differences of 2.7% for chitosan and 41.9% for gold microparticles. Detection of both cells in Polygon AI takes only 10 seconds, while cell counting in FIJI/ImageJ takes up to 253 seconds. A combination of both analytical and artificial intelligence programs is needed to combine both their advantages to produce reliable results.*

Keywords*: microscopy, image analysis, polygon AI, FIJI-image J, cellular structures*

I. INTRODUCTION

Microscopy is an essential characterization tool utilized in numerous fields such as engineering and biology. It can be used to describe the microstructure of polycrystalline materials and measure the average grain size which can be related to strengthening by grain refinement mechanism. Microscopy is utilized to research ways to create better innovative and technologically advanced materials and devices with lower mass, smaller volume, higher efficiency, and lower cost. In biomedicine and biotechnology, microscopes of various complexities help in pathology, drug delivery, cell characterization and more.

Light microscopy is one common type of microscopy with resolution that is matched to the sizes of cellular to subcellular structures. In fluorescence microscopy, a wide variety of fluorescent probes are available to mark proteins, organelles, and other structures for imaging. The relatively non perturbing nature of light allows for long-term imaging of living cells to monitor their dynamics. Other types of microscopies include nonlinear optical microscopy (NLOM) techniques to examine tissue non-invasively without labeling at depths not accessible

with traditional microscopy methods. Others utilize both 2-photon fluorescence (2-PF) and second harmonic generation (SHG) imaging using autofluorescence and fluorescence-labeled tissues and biomaterial structures [1, 2, 3, 4].

Research in microscopy often includes reporting the cell count in a particular area viewed under the microscope. To aid the researchers from manually counting all the cells in numerous images, advanced software such as FIJI/ImageJ, CellProfiler, Grid cell counter, and MetaMorph are used for cell counting. However, more advanced methodology is necessary to improve on 1) accuracy, 2) automation of the analysis and decision-making process and 3) large data volume processing. Hence, independent developers program external tools, known as third-party plugins, compatible with available programs such as FIJI/ImageJ to add features addressing specific needs, and even integrating artificial intelligence to further streamline specific tasks [5, 6].

An example of a third-party AI plugin is PIPSQUEAK for FIJI/ImageJ. It was developed in 2016 by the Rewire AI team, founded by Dr. John Harkness at Washington State University. The goal of the plugin is to facilitate automated cell detection and cell counting by encapsulating the target cells inside region of interest (ROIs) borders based on their shape and brightness or intensity values. The plugin can detect these due to extensive training of AI-driven detection-based image identification models using Rewire AI team's tool, Sightologist [7].

The models for PIPSQUEAK were trained based on thousands of cell images using different image staining techniques, six of which include Parvalbumin, c-Fos, Somatic, Microglia Cortex, DAPI and WFA staining. In the current version of PIPSQUEAK, these image models come as pre-trained options to aid in the researcher's analysis. Further developments of PIPSQUEAK allow for the researchers to send their newly detected cells to be trained as a customized model separate from the pre-trained models [8].

Eventually, Polygon AI was developed as an offshoot to the PIPSQUEAK plugin by evolving into a stand-alone application separate from FIJI/ImageJ. Polygon AI is intended as a software for biomedical image analysis. Because of its earlier usage in biomedical image analysis, it has developed high accuracy in detecting cells and features in tissues, examples of these are c-Fos, DAPI, Microglia Cortex, Parvalbumin, WFA, and Somatic cells. Each of these have their own specific image characteristics. In Figure S1, the contours show examples of these images and a description of each.

The objective of this study is to determine the applicability of an AI model that has been trained on biomedical components for detection and measurement of inorganic/organic nano- and micro-sized materials. This will widen the application of Polygon AI and enable image analysis of nanomaterials to be done through an integrated AI software that is already available. The anticipated benefit is to have rapid transition to the necessary applications using already available tools. This will be done through a comparison of Polygon AI as an imaging analysis tool compared to existing software such as FIJI/ImageJ by comparing its accuracy and speed when detecting the regions of interest (ROIs). The test structures are micron-sized particles of synthesized chitosan and gold agglomerates. Through this study, we aim to gain a

better understanding of AI image analysis comparing its output with programs requiring more human input.

II. METHODOLOGY

Figure 1 illustrates the schematic that summarizes the flow of the methodology from the image analysis and synthesis, which are further described in the next sections. Two images, each representing a different cell type, were manually counted. These counts served as a benchmark to compare the cell detection accuracy of the recommended and custom models, and to assess the impact of image processing adjustments on ROI outputs.

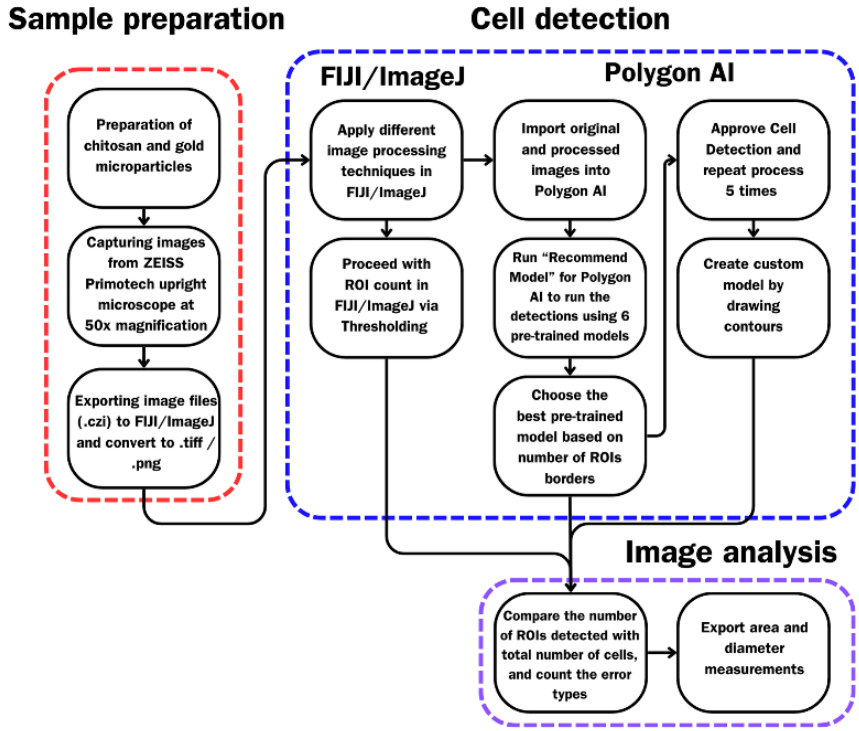

Figure 1: Schematic of the methodology for image analysis of chitosan and gold microparticles

1. Image Analysis

There are two main programs studied in this work. ImageJ is the standard image analysis program where the shape, count, dimension, histogram of data can be taken through initial modification of the parameters. These adjustments are verified by an operator. The program Polygon AI was used as the AI-based processor [7].

a. FIJI/ImageJ

FIJI, an enhanced version of ImageJ, offered additional plugins tailored for microscopy researchers. This program was used to process the images taken with the microscope. To prepare the image for ROI counting, the "Threshold" tool was used to select cells by

highlighting the bright intensity values of pixels in an image, which are usually contrast to the dark pixel values of the background. ImageJ's Threshold/Binary or color-balance features enabled modification and inversion of color or contrast of the images before importing them to Polygon AI, where the "Binary" tool converts pixel values into two different values, 0 for dark / black values and 255 for white values, depending on the original pixel values of the imported image. This step also helped in the detection of the ROIs within FJI/ImageJ. Another image processing method is by image inversion. An "Inverted" image is where the dark pixels are converted to lighter values and vice versa. It is adjusted by combining the image stack and adjusting the color balance in FIJI/ImageJ. Additionally, image splitting was applied to divide large images into smaller sub images to potentially enhance the ROI detection accuracy by reducing errors such as overlapping ROIs or merged cells. Figure 2 illustrates the types of processing applied to the images using FIJI/ImageJ.

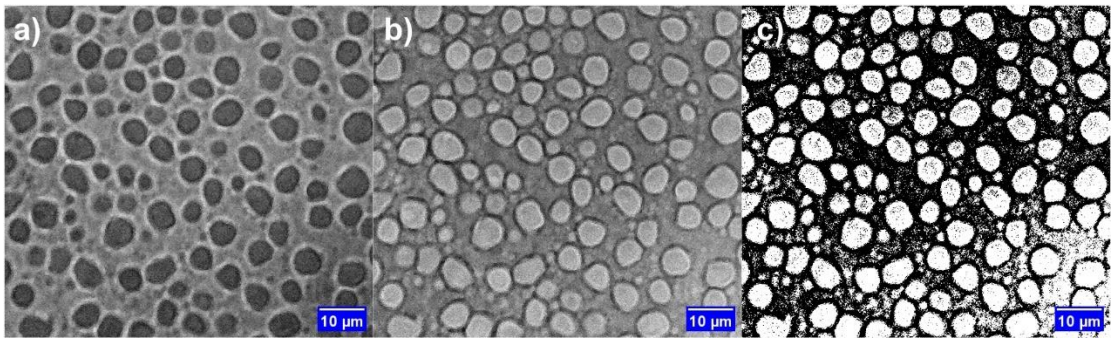

Figure 2: a) Original image and image after the processing methods b) Inverted and c) Binary.

b. Polygon AI

Upon installation, users are prompted to create an account for synching images to Rewire AI's server. The user interface featured a gallery for importing image files and a detection area where built-in models could be selected to identify cells in the images (Figure S2). Different image processing methods were compared to check if Polygon AI can correctly count and identify all the cells compared to that of a manual count, where the types of processing applied differ by their resulting intensity values seen in Figure 2. Users could enable the "Recommend Model" option from a drop-down menu, allowing Polygon AI to scan the different images through six main built-in models.

Two key settings were available: Detection Sensitivity and Overlap Removal. Increasing Detection Sensitivity allowed for the detection of more cells. This is done as an adjustment if the initial run with the default setting were unable to detect actual ROIs. Increasing Overlap Removal helped eliminate overlapping ROIs, which often occurred with string-like shaped cells.

The errors in cell detection were evaluated by counting the number of ROIs that Polygon AI detected compared to the manual count. Different error types were defined, as shown in Figure 3, as follows: a False Positive was when the ROI outline, in red dashed-line, was present but did not contain the cell, in orange, or did not fully enclose the cell within its ROI, a False Negative was when there was a cell without an ROI, an Overlap Type I was when

more than one ROI captured one cell, and an Overlap Type II was when one ROI captured more than one cell. Errors were determined based on these classifications, and the occurrences of each were noted. Users selected the most suitable model, upon initial exploration of the models. The model with the highest number of ROIs detected and the least errors (false positives and false negatives) are selected.

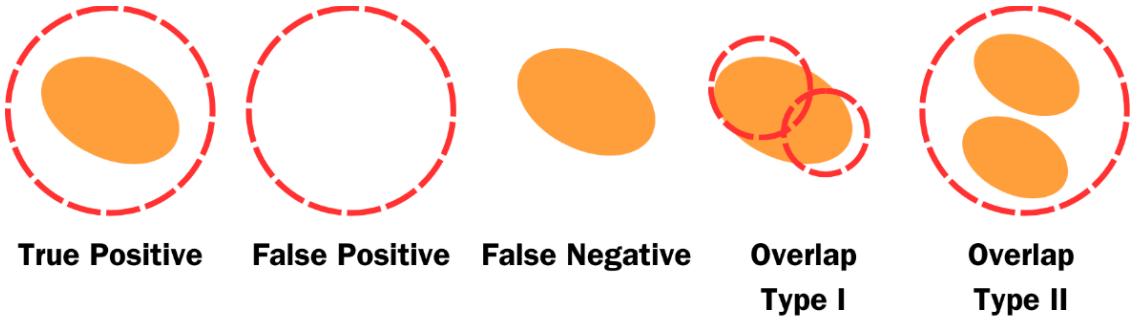

Figure 3: Error detection types during cell counting in Polygon AI

When detection errors occurred, ROIs were deleted after the model completed its analysis and images were re-analyzed using another model. Additionally, custom model training was available to create models for specific cell types as mentioned in the introduction. A custom model is defined by teaching the AI of the features of the specific samples – chitosan and gold. This involved feeding the AI with many images so that it will be able to identify a similar ROI. The aim of using Custom Modeling within Polygon AI is to enable better detection of structures that have not been trained as one of the built-in models, which should result in better and faster ROI detection. In Polygon AI, custom models are trained by selecting at least five photos detected using one built-in model and their ROIs approved after detection. Once selected, at least 20 contours of the cell inside the ROI are manually drawn to follow the shape of the cell as well as detect their image contrast (see Appendix 3 Figure S1 in the supplementary information). For this experiment, a total of 8 custom models were trained by varying the images used for training, two of which included creating models from imported ROIs made in FIJI/ImageJ. The ROIs used were processed through previous imaging processing methods discussed earlier. Figure S1 illustrates a custom model being trained using the minimum 5 annotated images with 20 contours.

c. Laboratory Image Analysis Procedure

The tools used for running both programs included a computer with 16GB RAM and an 8-core 3.3 GHz. FIJI/ImageJ and Polygon AI were installed. Around 5GB worth of storage was needed for storing image files and for the programs. Other equipment used was the ZEISS Primotech upright microscope (.czi for Zeiss Microscopes). The image files (.czi) were converted to (.tiff) before analysis. Experimental limitations include the available microscope lens magnification of 50x and the free license of Polygon AI, which only allows two (2) custom models per account. A timer was used to measure the duration of the processes of the detection of the ROIs as well as the creation of the custom models. After image analysis in Polygon AI, the ROIs are approved, and the data can be exported into a .csv file, and the values of the diameter are reported.

2. Synthesis

The model "cell-like" structures were micron-sized chitosan particles. To synthesize them, a solution of chitosan (CS) in acetic acid (AA), was mixed with a solution of the cross-linking agent sodium triphosphate (TPP) following the procedure by Raguindin et al. [9]. Samples of the chitosan and acetic acid solution (CS + AA), each 10ml were prepared. The cross-linking agent TPP (3mL, 6mL, 10mL) was added immediately and stirred for another 5 minutes at 700 rpm. After stirring, the droplets of the solutions were set onto glass slides to set for microscopy.

The gold microparticles were synthesized via reduction of Au+3 in a solution of chlorauric acid sodium thiosulfate as described in the paper by Otero et al. [10]. The initial nanoparticle solution was kept in the dark at room temperature for 24 h for the aggregation of nanoparticles to proceed in solution. After this, a murky brown-purple solution was formed. This was dropped into glass slides and dried in the laboratory environment.

The glass slides with gold nanoparticles were imaged with the Zeiss microscope as described in the following section.

III. RESULTS AND DISCUSSION

Chitosan particles of various sizes were formed by increasing amounts of TPP. A small amount of TPP resulted in long, flaky chitosan particles, while a larger amount resulted in small, nodular particles. Images of these particles were taken and analyzed using Image J and Polygon AI.

FIJI-processed images were loaded into Polygon AI with the initial "Recommend Model" detection settings for chitosan cells and gold microparticle images (Detection Sensitivity = 75, Overlap Removal = 25). Only three of the six models detected regions of interest (ROIs). Two models captured less than 15% of the total cells in the images, based on manual counts. Further experiments in image processing, such as cropping images and adjusting pixel intensity and contrast, were conducted to improve detection. After cropping, the images were re-analyzed with Polygon AI, and the same three models detected cells. The results are discussed in the following sections.

1. Using pre-set models in Polygon AI

The models that successfully detected chitosan cells were DAPI, Microglia Cortex, and Somatic. The models that failed to detect cells were Parvalbumin, c-Fos, and WFA. From the three models that detected the cells, the Somatic model closely captured most of the chitosan cells and gold microparticles compared to the DAPI and Microglia Cortex models. This was due to the chitosan cells closely resembling Somatic cells, which are known as the simplest body cells with the complete number of chromosomes [11]. According to the research of Zajác et.al, the Somatic cells found in raw cow's milk closely resembled the shape of the chitosan

and gold cells (Figure 4) [12]. Since the Somatic model was also able to identify both the chitosan and gold microparticles from the initial Recommend Model scan, it was used to test the detection of cells with different image processing methods and for subsequent custom model training.

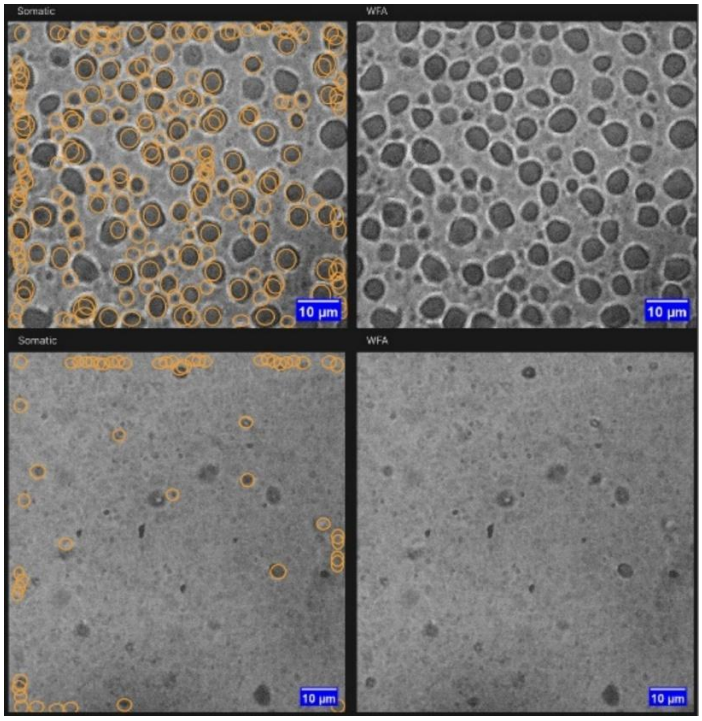

Figure 4: Sample Polygon AI ROI detection results using the "Recommend Model" option for a) Chitosan and b) Gold Microparticles using Somatic (left) and WFA (right) models.

Table 1 shows the ROI detection results of chitosan cells using the different image processing methods. From a manual count, the total number of chitosan cells in the image is 105. The imaging process method that performed the best is performing a Binary method and splitting the images, which resulted in a difference of 2.86% from the original count, followed by the Binary method on not splitting the images with a difference of 4.76%. The worst performing method is splitting the original image, which resulted in a 55.24% difference and reported up to 76 False Positive ROIs and 67 False Negatives. In comparison to FIJI/ImageJ, the best imaging processing method in Polygon AI detected 17% more ROIs and is likely due to the errors in processing such as merged cells and cells along the edges in FIJI/ImageJ.

Table 1: Summary of the detection of Chitosan cells using the Somatic model with different image processing methods applied before running Polygon AI analysis

Method Type		Total ROI Count (b)	False Positive	False Negative	Overlap Type I	Overlap Type II	True Positive (c)	Total ROI Counted vs Manual Count =b/a	Total True Positive vs Manual Count =c/a	Remarks
Manual count		**105** (a)	-	-	-	-	-	-	-	
FIJI/ImageJ		87	0	18	-	-	87	82.86%	82.86%	
Not Split	Original	153	63	18	3	0	87	145.7%	82.86%	
	Inverted	125	23	7	4	0	98	119.04%	93.33%	Overcount
	Binary	121	9	5	12	0	100	115.2%	95.24%	Overcount; second highest true positive; lowest errors
Split	Original	124	76	67	1	0	47	118.09%	44.76%	Overcount
	Inverted	123	32	33	21	0	72	117.14%	68.57%	Overcount
	Binary	125	19	3	4	0	102	119.04%	97.14%	Overcount; highest true positive

Legend: *Original:* No image processing was applied to the image*; Invert:* The values are inverted; dark pixel values turn light and vice versa*; Binary:* Only black and white values are rendered, where black is the background color and white is the cell color; *Split:* Images are split to more than one image*; Manual Count:* Cells are counted by hand, *ROI:* Regions of Interests outlines that enclose the cell*; False Positive:* ROI present without cell inside*; False Negative:* Cells without ROI*; Overlap Type I:* Cell with 2 or more ROIs*; Overlap Type II:* ROI with 2 or more cells

In the analysis of gold particles, through manual counting, the total number of microparticles in the image was determined to be 21, see Table 2. Applying the image processing methods, the imaging process method that performed the best is Binary method and it did not depend on whether the image was split or not. This resulted in a difference of 33% from the original count. The worst performing method is splitting the inverted image, which resulted in a 319.05% difference and reported up to 64 False Positive ROIs. However, the latter model was the most accurate in terms of the number of True Positive ROIs detected, with a difference of 9.52%. In comparison, FIJI/ImageJ reported a lesser difference of 19.05% of detected ROIs compared to the Binary method reporting 33% difference. In terms of the number of True Positive ROIs, the Split Inverted fared better than the 19.05% difference of FIJI/ImageJ.

Table 2: Summary of the detection of Gold microparticles using the Somatic model using different image processing methods applied before running Polygon AI analysis

	Method Type	Total ROI Count (b)	False Positive	False Negative	Overlap Type I	Overlap Type II	True Positive (c)	Total ROI Count vs Manual Count = b/a	Total True Positive vs Manual Count = c/a	Remarks
	Manual count	**21** (a)	-	-	-	-	-	-	-	
	FIJI/ImageJ	17	0	4	0	0	17	80.95%	80.95%	
Not Split	Original	54	42	11	2	0	10	257.14%	47.62%	Overcount
	Inverted	34	26	14	1	0	7	161.90%	33.33%	Overcount
	Binary	14	2	10	1	0	11	66.6%	52.38%	
Split	Original	76	62	11	3	0	10	361.90%	47.62%	Overcount
	Inverted	88	64	2	5	0	19	419.05%	90.48%	Overcount
	Binary	28	13	6	0	0	15	133.33%	71.43%	Overcount

Legend: same as Table 1.

2. Custom Models in Polygon AI

The custom model for chitosan cells that produced the closest ROI detection was the one created using Binary images resulting in a 17.14% difference from the manual count. However, upon closer inspection of the images, all models only detected less than 4% of the chitosan cells. From the errors, the model using the original images produced the most amount of False Positive ROI detections with a count of 130, while the inverted model produced the least amount with 96. Overlap errors were also prevalent with 27 counts seen at the inverted model, whose ROI captures more than 3 cells with the ROI. The custom model for gold microparticles that produced the closest ROI detection was the Binary model resulting in a 33.33% difference from the manual count, and its model detected 11 of 21 True Positive ROIs. The inverted model detected the most ROIs, yet only one True Positive ROI was correct with 2 Overlaps present. Based on the results, the built-in Somatic model is better at detecting True Positive ROIs of chitosan particles compared to the custom models trained from actual pictures of chitosan particles. As seen in the images, the ROIs fail to fully enclose the cell, which ranges less than 50% of the target cell captured. From there, the minimum of 5 images and 20 contour drawings is not enough for the custom model to accurately capture the chitosan cells and gold microparticles. Figure 5 illustrates the detections of the custom models for both chitosan and gold microparticles.

Table 3: Summary of the detection of Gold microparticles using the Custom model using different image configuration

Cell Type	Custom Model Type	Total ROI Count (b)	False Positives	False Negatives	Overlap Type I	Overlap Type II	True Posi-tive (c)	Total ROI Count vs Manua-l Count = b/a	Total True Positive vs Manual Count = c/a	Remarks
Chito -san	Manual count	105 (a)	-	-	-	-	-	-	-	-
	FIJI/ ImageJ	140	127	101	0	9	4	133.33%	3.81%	x
	Original	145	130	103	7	6	2	138.10%	1.90%	x
	Inverted	133	96	102	7	27	3	126.67%	2.86%	x
	Binary	123	110	102	1	9	3	117.14%	2.86%	x
Gold	Manual count	21 (a)	-	-	-	-	-	-	-	
	FIJI/ ImageJ	14	2	10	1	0	11	66.66 %	52.38%	
	Original	41	38	19	0	1	2	195.24%	9.52%	
	Inverted	55	52	20	0	2	1	261.90%	4.76%	
	Binary	14	2	10	1	0	11	66.66 %	52.38%	

Legend: Same as Table 1; x = over detection and under detection errors are too large

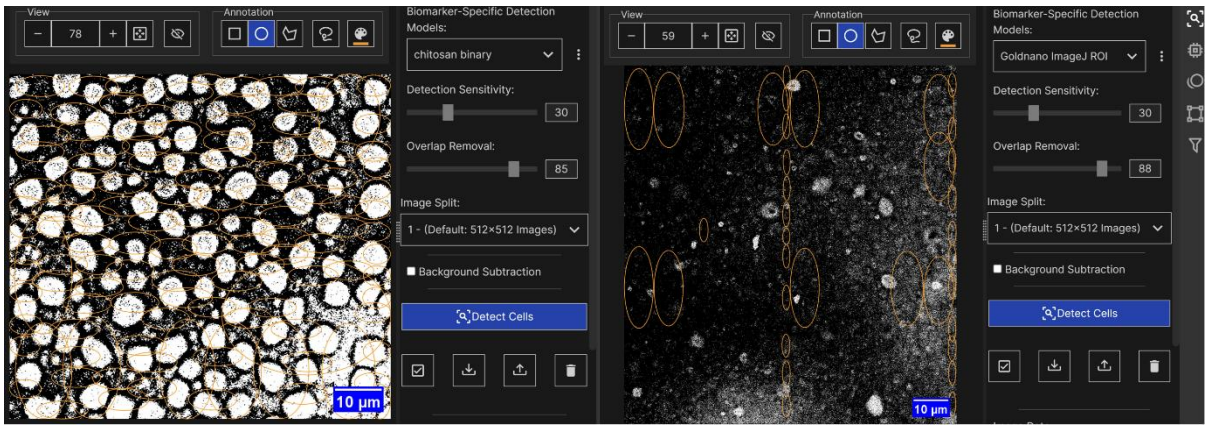

Figure 5: Sample ROI detection results of Chitosan particles (left) and Gold microparticles (right) after running through custom trained models

3. Measurements of ROIs

After the ROIs are detected, the software allows for data of the cell from the ROIs to be exported. Measurements include the area and diameter of the cell, circularity, mean

intensity, and others. Area and diameter values are reported in pixels, but it is possible to convert these values in terms of micron, should the microscope image file present a conversion unit of the number of pixels per micron. Diameter measurements of chitosan cells and gold microparticles from both FIJI/ImageJ and Polygon AI are compared, see Table 4. The difference between the average values of the chitosan cells is 2.7% and 41.9% for gold microparticles. The larger percent difference with the gold microparticles is due to Polygon AI considering the size of the ROI instead of encapsulating the actual shape of the cell, where in the case of FIJI/ImageJ's ROIs take the shape of the cell.

Table 4. Measurements of particles using both programs

	Mean, µm	**Median, µm**	**Mode, µm**
Polygon AI - Chitosan	5.2	5.09	5.04
Image J - Chitosan	5.06	5.17	5.04
Polygon AI - Gold	3.89	3.91	4.26
Image J - Gold	2.74	2.82	3.15

The time taken to accomplish the ROIs was measured and recorded. Manual counting of 105 ROIs took 63 seconds. Using FIJI/ImageJ, identifying the ROIs took between 210 to 253 seconds. In three trials with different pictures of chitosan cells, the fastest time for Polygon AI to process the with the Recommend Model option enabled was 27 seconds, while the longest was 51 seconds. Detecting the ROIs of one image using the pre-trained models took an average of 10 seconds. For custom modeling, it took 50 seconds to approve 5 images with ROIs, followed by an additional 480 seconds for editing and 420 seconds to draw at least 20 contours. The entire process took at least 16 minutes or 960 seconds. Another 15 minutes were needed for the server to train the model, totaling 30 minutes to create a custom model from scratch. Models trained longer if more images were added, and more contours were drawn. If imported FIJI/ImageJ ROIs were used, an additional 18 minutes were required to have 5 images with ROIs.

Table 5: Time durations of methods for cell counting of 105 chitosan cells

Method	**Time (s)**
Manual Count	63
FIJI/ImageJ Method	210 -253
Polygon AI - Pre-trained Model (Somatic)	10
Polygon AI - Custom Model Method	1800

The advantages of using FIJI/ImageJ include its ability to capture a cell's contour for counting. However, the process is time-consuming due to the necessary image processing steps to adjust the intensity values of the cells for better counting. Additional processing is required for further accuracy, such as erasing unwanted pixels. Furthermore, individual cells sometimes merge after processing them into binary form, and applying a watershed technique can help correct this error.

Polygon AI offers a simpler process and quicker detection of ROIs. However, time is still spent adjusting the Detection Sensitivity and Overlap Removal values, as well as post-processing ROIs by deleting and resizing incorrect ones. Time is also needed for approving the ROIs and drawing the contours from them. From the experiments, the built-in Somatic model for cell detection performed better at detecting chitosan cells and gold microparticles compared to the custom models.

This paper focused on chitosan and gold nanoparticles because these are some representative materials for various shapes and contrasts of images of inorganic/organic microscopic particles. The particles tested were all rounded, spherical, or oblong in shape. This is seen to be the reason for the relatively good results in Somatic model. Detection of irregularly shaped particles have not been done due to difficulty in obtaining submicron sized particles with large length to width ratio. However, it is anticipated that the applicable model will also change with shape.

IV. CONCLUSIONS AND RECOMMENDATIONS

Polygon AI could detect and count cell-like structures or particles from microscope images. However, consideration of the type of models, detection sensitivity, overlap removal, coloration, and image splitting required more human input to achieve accurate results. For the most accurate detection of chitosan particles, the image should be converted to Binary mode before running it through Polygon AI, using the Somatic model. Splitting the images yielded higher accuracy. The most accurate detection of gold microparticles was achieved by using the Inverted method before running them through Polygon AI, also with the Somatic model and by splitting the images. Custom model training, which involved the minimum requirement of annotated images and contours, led to inaccurate detection and took longer.

Creating custom models took longer due to the need to draw individual contours and wait for the model to be ready. These custom models detected too many ROIs that were neither chitosan cells nor gold microparticles, unlike the available Somatic model in Polygon AI, which led to more accurate results.

FIJI/ImageJ, despite being a reliable tool for detecting and measuring ROIs, was quite time-consuming due to the need for adjustments tailored to each image. Polygon AI, meanwhile, was limited due to its requirement for large quantities of sample images and ROIs for the custom model training to work properly. Additionally, the relatively good counting of micro-particles using the Somatic model showed that image analysis can be done without prior sample treatment like staining. Therefore, to combine these advantages, researchers could best use Polygon AI's built-in model for counting cells, while FIJI/ImageJ could be used to measure the diameter readings of the cells.

V. ACKNOWLEDGEMENTS

This work was supported by the Department of Science and Technology MECO-TECO Joint Research Project. TAAH and CJMK were supported under the Philippine Science High School Science Immersion Program.

References:

[1] Solomon CV. 2022. On the role of microscopy in mechanical engineering education. Microscopy and Microanalysis. 28(S1):2954-2956.
[2] Rydz J, Šišková A, Eckstein AA. 2019. Microscopic techniques in materials science: Current trends in the area of blends, composites, and hybrid materials. Advances in Materials Science and Engineering. 1:9072958.
[3] Araki T. 2017. The history of optical microscope. Mechanical Engineering Reviews. 4(1):16-00242.
[4] Thorn K. 2016. A quick guide to light microscopy in cell biology. Molecular Biology of the Cell. 27(2):219-222.
[5] Vielreicher M, et al. 2013. Taking a deep look: Modern microscopy technologies to optimize the design and functionality of biocompatible scaffolds for tissue engineering in regenerative medicine. Journal of the Royal Society Interface. 10(86):20130263.
[6] Diaspro A, Chirico G, Collini M. 2005. Two-photon fluorescence excitation and related techniques in biological microscopy. Quarterly Reviews of Biophysics. 38(2):97-166.
[7] Schindelin J, et al. 2012. Fiji: an open-source platform for biological-image analysis. Nature Methods. 9(7):676-682.
[8] Reinhard SM, et al. 2019. Reduced perineuronal net expression in Fmr1 KO mice auditory cortex and amygdala is linked to impaired fear-associated memory. Neurobiology of Learning and Memory. 164:107042.
[9] Raguindin RKM, Mercado CC. 2022. A micro-composite prodrug and its theranostic potential. AIP Conference Proceedings. AIP Publishing. 2440:1.
[10] Otero CM, et al. 2022. Optimized biocompatible gold nanotriangles with NIR absorption for photothermal applications. ACS Applied Nano Materials. 5(1):341-350.
[11] Polak JM, Bishop AE. 2006. Stem cells and tissue engineering: past, present, and future. Annals of the New York Academy of Sciences. 1068(1):352-366.
[12] Zajac P, et al. 2016. Fluorescence microscopy methods for the determination of somatic cell count in raw cow's milk. Veterinární Medicína. 61:11.